Food Research International 164 (2023) 112441

Contents lists available at ScienceDirect

Food Research International

journal homepage: www.elsevier.com/locate/foodres

^{1}H NMR-based metabolic profile and chemometric analysis for the discrimination of *Passiflora* species genotypic variations

Livia Macedo Dutra [a,*], Pedro Henrique Vieira Teles [a], Alan Diego da Conceição Santos [a,b], Natoniel Franklin de Melo [c], Noemi Nagata [d], Jackson Roberto Guedes da Silva Almeida [a,*]

[a] Center for Studies and Research of Medicinal Plants (NEPLAME), Federal University of San Francisco Valley, 56304-205 Petrolina, PE, Brazil
[b] Chemical Research Group of Amazon Micromolecules (NEQUIMA), Federal University of Amazonas, Manaus 69077-000, AM, Brazil
[c] Brazilian Agricultural Research Corporation (EMBRAPA), Embrapa Semiárido, 56302-970 Petrolina, PE, Brazil
[d] Department of Chemistry, Federal University of Paraná, 81530-900 Curitiba, PR, Brazil

ARTICLE INFO

Keywords:
Passiflora
^{1}H NMR
Chemometrics
Metabolic profile
Biological activities
Quality control

ABSTRACT

The species of the genus *Passiflora* (Passifloraceae family) have been used as food, cosmetic and traditional herbal. As a result, the *Passiflora* species are widely cultivated and has an economic, medicinal and ornamental importance. The popular designation as "passion fruit" and chemical profile of several *Passiflora* species remains unknown. The lack of chemical information contributes to the erroneous classification and adulteration. In recent years, special attention has been paid to the bioactivity and phytochemical profiles of several *Passiflora* species extracts. In this research, ^{1}H NMR-based metabolic profiling coupled with chemometric tools was used to characterize and distinguish extracts obtained from different wild *Passiflora* species (*P. alata*, *P. cincinnata*, and *P. setacea*) and genetic varieties (*P. alata* var. BRS Pérola do Cerrado, *P. cincinnata* var. BRS Sertão Forte, and *P. setacea* var. BRS Pérola do Cerrado). Fourteen metabolites were identified by 1D and 2D NMR experiments, highlighting the presence of fatty acids, carbohydrates, saponins, alkaloids, and mainly C-glycosidic flavones. Principal components analysis (PCA) allowed discrimination of *Passiflora* extracts, which the quadranguloside, oleanolic acid-3-sophoroside, α-glucose, β-glucose, and vitexin-2-*O*"-rhamnoside were relevant in the differentiation of *P. alata* and *P. alata* var. BRS Pérola do Cerrado, while the flavones isovitexin and isovitexin-2-*O*"-xyloside were dominant in the grouping of *P. setacea* and *P. setacea* var. BRS Pérola do Cerrado, and finally *P. cincinnata* and *P. cincinnata* var. BRS Sertão Forte grouped by the influence of the fatty acids, sucrose, flavones (isoorientin and vitexin-2-*O*"-xyloside), and trigonelline. The varieties of *P. setacea*, and *P. cincinnata* are chemically equivalent to the original *Passiflora* species. However, the PCA analysis showed that the genetic variety of *P. alata* occupied a different position in the scores plot provoked mainly by the presence of oleanolic acid-3-sophoroside. The ^{1}H NMR metabolic profile can be efficient for quality control evaluation, and can contribute to the investigation of new alternatives for official *Passiflora* herbal medicines.

1. Introduction

Passiflora L. belongs to the Passifloraceae family and comprises by almost 630 species. Its occurrence is described mostly in Tropical America with parallel reports in Australia, China, India, and the Pacific Islands (Faleiro et al., 2019; Pereira, Lima, Soares, Laranjeira, de Jesus, & Girardi, 2019). About one hundred and fifty *Passiflora* species, popularly known as "passion fruit", are originally from Brazil, some of which has been widely employed in food, cosmetic, and pharmaceutical industries (Patel, Soni, Mishra, & Singhai, 2011; Pereira et al., 2019). In 2020, Brazil produced 690,364 t of *Passiflora* fruit, with a great participation of the Northeastern region contributing with 71.17% of the production (IBGE, 2020). Among *Passiflora* species, *Passiflora edulis* Sims. is the most cultivated one and can be found in 90% of the orchards. *P. edulis* is commonly consumed as fresh fruit or used for producing juices, beverages, jams, sweets, and jellies (Faleiro et al., 2019). Other species economically important in Brazil are *Passiflora alata* Curtis, *Passiflora cincinnata* Mast., *Passiflora setacea* DC., and their genetic varieties have also achieved commercial interest due to their edible fruits and medicinal appeal (Bomtempo, Costa, Lima, Engeseth, & Gloria,

* Corresponding authors at: Federal University of San Francisco Valley, 596304-205 Petrolina, PE, Brazil.
E-mail addresses: liviadutranmr@gmail.com (L.M. Dutra), jackson.guedes@univasf.edu.br (J. Roberto Guedes da Silva Almeida).

https://doi.org/10.1016/j.foodres.2022.112441
Received 10 October 2022; Received in revised form 26 December 2022; Accepted 29 December 2022
Available online 2 January 2023

2016; Faleiro et al., 2019). The genus *Passiflora* has contributed significantly to plant breeding programs, since most species have longevity, tolerance to diseases, pests and hydric stress, as well as high concentrations of important pharmaceutical industry metabolites, such as flavonoids (Bernardes et al., 2020; Bomtempo et al., 2016; Wosch, dos Santos, Imig, & Santos, 2017).

Traditionally, *Passiflora* species have been indicated for the treatment or prevention of disorders of central nervous system, such as depression, insomnia, and anxiety (Figueiredo et al., 2016). Biological studies have shown analgesic (He et al., 2020; Sasikala, Saravanan, & Parimelazhagan, 2011), anti-inflammatory (Patel et al., 2011; Sasikala et al., 2011), antibiotic (Siebra et al., 2018), antioxidant (Shanmugam et al., 2020; Wasicky et al., 2015), anti-diabetic (He et al., 2020; Shanmugam et al., 2020), gastroprotective (Wasicky et al., 2015), sedative (Gazola et al., 2018; He et al., 2020), anxiolytic (Holanda et al., 2020), and anticonvulsant effects (Holanda et al., 2020) in the genus *Passiflora*. Although several *Passiflora* species are often used for medicinal purposes, only *P. edulis* Sims and *P. alata* Curtis are included in the 6th Edition of the Brazilian Pharmacopoeia (Anvisa, 2019). Recently, *Passiflora incarnata* was added to the 2nd Edition of the Form of Herbal Medicines of the Brazilian Pharmacopoeia (Anvisa, 2021; Fonseca, 2020). Several pharmacological and taxonomic investigations on *P. alata* and *P. edulis* have been performed. However, other *Passiflora* species native to Brazil, albeit cataloged a long time, have been neglected and there is no information on their potential uses as food, cosmetics, and pharmaceuticals (Fonseca, 2020).

In addition, *Passiflora* spp. present numerous classes of chemical compounds, with emphasis on alkaloids (Bomtempo et al., 2016; Dhawan, Dhawan, & Sharma, 2004), saponins (Doyama, Rodrigues, Novelli, Cereda, & Vilegas, 2005; Reginatto et al., 2001), terpenes (Ozarowski, Piasecka, Paszel-Jaworska, & de Chaves, 2018; Reginatto et al., 2001), and phenolic compounds (Dhawan et al., 2004; Patel et al., 2011), mainly C-glycosylated flavonoids derived of the apigenin and luteolin (Gazola et al., 2018; McCullagh, Goshawk, Eatough, Mortishire-Smith, Pereira, Yariwake, & Vissers, 2021; Ozarowski et al., 2018).

In this regard, analytical tools associated with chemometric have enabled simultaneous identification and quantification of primary and secondary metabolites via metabolic profiling or fingerprint approaches in several medicinal plants, including *Passiflora* species (Danek, Plonka, & Barchanska, 2021; Dutra et al., 2020; Emwas et al., 2019; Farag et al., 2016; Hellal, Mediani, Ismail, Tan, & Abas, 2021). Mass spectrometry (EM) - coupled with liquid (LC) or gas (GC) chromatography - and nuclear magnetic resonance (NMR) are the main analytical techniques employed in this area (Emwas et al., 2019). Among the advantages of using NMR stand out the speed and simplicity of samples preparation, the possibility of identify and quantify multiple metabolites at the same spectrum, high reproducibility, and the non-destructive aspect of this technique (Brahmi et al., 2020; Dutra et al., 2020; Farag et al., 2016; Hellal et al., 2021; da Santos, 2018; Snyder, 2021).

Assessing the chemical composition of plants with biological and economical importance, as *Passiflora*, is essential. In this sense, untargeted metabolic profiling can be very helpful offering the opportunity of tracking major and minor metabolites. Furthermore, there is a great interest in developing methods to efficiently identify and distinguish *Passiflora* species, their genetic varieties, as well as to discriminate species according to applications and popular uses. Also, adulteration and misidentification can impact the commercial values of *Passiflora* species and affect their therapeutic application (Brahmi et al., 2020; Fonseca, 2020). In this context, Farag et al. (2016) and Flores, Martinelli, and Lião (2020) proposed ^{1}H NMR metabolic fingerprint approaches for both differentiation of geographic origins and quality control of some *Passiflora* based on herbal medicines (Farag et al., 2016; Flores et al., 2020).

Herein, we employed ^{1}H NMR-based metabolic profiling associated with chemometric analysis to differentiate *Passiflora* species (*Passiflora alata* Curtis, *Passiflora cincinnata* Mast., and *Passiflora setacea* DC.) and their genetic varieties by comparing the chemical composition of the *Passiflora* extracts. This investigation can contribute to quality control and help investigate alternatives for the official herbal medicines of *Passiflora*.

2. Material and methods

2.1. Chemicals and reagents

All the chemical reagents were of analytical grade. Dimethyl sulfoxide-d_6 (DMSO-d_6, 99.9% ^{2}H) containing tetramethylsilane (TMS, 0.03%) was purchased from Cambridge Isotope Laboratories, Inc. (Massachusetts, USA). Absolute ethanol was supplied from LabSynth (São Paulo, Brazil) and distilled water was acquired in our laboratory.

2.2. Samples collection and preparation

Leaves of wild *Passiflora* species (*Passiflora alata* Curtis, *Passiflora cincinnata* Mast., and *Passiflora setacea* DC.) were collected in August 2019, while their varieties (*Passiflora alata* Curtis var. BRS Mel do Cerrado, *Passiflora cincinnata* Mast. var. BRS Sertão Forte, and *Passiflora setacea* DC. var. BRS Pérola do Cerrado) were obtained in August 2018. All *Passiflora* samples were stored at Brazilian Agricultural Research Corporation (EMBRAPA) Semiarid, housed in Petrolina city, Pernambuco State, Brazil. *Passiflora* spp. were dried in an oven of circulating air at an average temperature of 45 °C for 72 h, and submitted to pulverization in an analytical mill (Quimis, São Paulo, Brazil) before the freezing. Afterward, the samples were kept at −20 °C until NMR data acquisition. All procedures for access to genetic patrimony and associated traditional knowledge were carried out and the project was registered in SisGen (Register #A1514EF).

2.3. Extraction of metabolites

Extractions were carried using about 50.0 ± 0.5 mg from the powder obtained from *Passiflora* spp. leaves in 1.0 mL of ethanol:water (7:3 v/v) in tubes, followed by sonication at 30 °C for 15 min in an SB-120DTN Ultrasonic Cleaner (Logen Scientific, São Paulo, Brazil). These samples were centrifuged at 4000 rpm for 10 min in a Universal 320R centrifuge (Hettich, Tuttlingen, Germany). The supernatant was collected and transferred to glass flasks and subsequently submitted to evaporation the solvent in an oven circulating air at 30 °C for 12 h, yielding *Passiflora* extracts. The powder was discarded. This procedure was realized in quintuplicate for each *Passiflora* species, resulting in 30 samples.

The sample preparation for NMR experiments was performed as previously described by Kim, Choi, and Verpoorte (2010) with adaptations. The extracts were dissolved in 500 μL of dimethyl sulfoxide-d_6 (DMSO-d_6) containing 0.03% tetramethylsilane (TMS) and added to 5 mm tubes for further NMR analyses.

2.4. NMR spectroscopic analysis

^{1}H NMR spectra were recorded at 298 K on a Bruker™ ASCEND III 400 NMR (Bruker BioSpin GmbH, Rheinstetten, Germany) operating at 9.4 T, observing ^{1}H and ^{13}C at 400 and 100 MHz, respectively. The NMR spectrometer was equipped with a 5-mm multinuclear direct detection probe (BBO probe) with *z*-gradient. The samples were locked on the deuterium signal from DMSO-d_6, and the magnetic field homogeneity was optimized for each sample. The ^{1}H NMR experiments were acquired using a water suppression pulse sequence, *zgpr* (Bruker library), in which the residual water signal at 3.411 ppm was eliminated. For each sample, 64,000 of time domain points for a spectral width of 24.99 ppm over 128 scans, radiofrequency pulse of 13.55 μs, acquisition time of 3.28 s, recycling delay of 2.0 s, 2 dummy scans, and 161 of receiver gain. The spectra were apodized via exponential Lorentzian broadening multiplication corresponding to 0.3 Hz line broadening in the transformed

spectrum, and zero filled to 64 k points prior to Fourier transformation. NMR spectra were referenced to TMS at 0.0 ppm. The total experiment time was 25 min for each sample, including the time required for locking, tuning and matching of the probehead, shimming, and acquisition procedure.

2.5. Metabolic profiling

The metabolite identity was assigned using one- and two-dimensional NMR experiments and in accordance with the literature (Abd Ghafar et al., 2020; Doyama et al., 2005; Farag et al., 2016; Ferreira et al., 2016; Gazola et al., 2018; Hosoya, Young, & Kunugi, 2005; Marchesine, Prado, Messiano, Machado, & Lopes, 2009; Zielińska-Pisklak, Kaliszewska, Stolarczyk, & Kiss, 2014), including online database, such as the Human Metabolome Database (HMDB) (Wishart et al., 2018). Thus, to support an unequivocal chemical shifts assignment in the ^{1}H NMR spectra, homonuclear correlation spectroscopy (^{1}H–^{1}H COSY), heteronuclear single quantum correlation (^{1}H–^{13}C HSQC), and heteronuclear multiple bond correlation (^{1}H–^{13}C HMBC) experiments were performed. Thus, the ^{1}H–^{1}H COSY experiment was obtained using *cosypgppqf* with spectral window of 6,410.3 Hz in both dimensions, 2,048 × 128 were acquired with 16 scans per increment and relaxation delay of 2.0 s. For ^{1}H–^{13}C HSQC, the *hsqcdetgpsisp2.3* sequence was used employed spectral window of 6,410.3 and 25,252.5 Hz in f2 and f1 dimensions, respectively, per 40 scans per increment, with an average coupling constant $^{1}J_{(C,H)}$ optimized for 145 Hz, relaxation delay of 2.0 s. ^{1}H–^{13}C HMBC experiment was performed with *hmbcgplpldqf* pulse sequence with coupling constant $^{LR}J_{(C,H)}$ of 8 Hz, 2,048 × 312, it was used 80 scans per increment, relaxation delay of 2.0 s, and spectral width of 6,410.3 in f2 and 25,252.5 Hz in f2 dimensions. The coupling constants (*J*) were expressed in Hz.

2.6. Chemometric analysis of the Passiflora species

The principal components analysis (PCA) was performed using AMIX® software (version 3.9.12, Bruker BioSpin, Rheinstetten, Germany). Firstly, all ^{1}H NMR spectra were manually phased, baseline corrected, and aligned with the use of the TopSpin® (version 4.0.9, Bruker BioSpin, Rheinstetten, Germany) software. The chemical shift range between δ 0.20–10.00 represented all ^{1}H NMR resonances in the samples. Such range was segmented in continuous small buckets with 0.05 ppm wide. The areas between 3.30 and 3.50 and 2.46–2.56 ppm were excluded from the ^{1}H NMR data to eliminate residual water and dimethylsulfoxide signals, respectively. The area under each bucket was integrated using the special integration mode. The spectra were scaled to the total intensity and after this procedure, a matrix was created in which each row represents the ^{1}H NMR spectra of the *Passiflora* samples and each column contains the integrated areas of the original signal within each bucket region. The quintuplicate of each sample resulted in a final matrix composed of 30 lines (samples) and 192 columns (variables or buckets). For the PCA analyses, autoscaling was employed as pre-processing. The identification of the metabolites responsible for the discrimination between species was performed through the loadings plot. The metabolites responsible for the variance data were attributed in comparison with the literature.

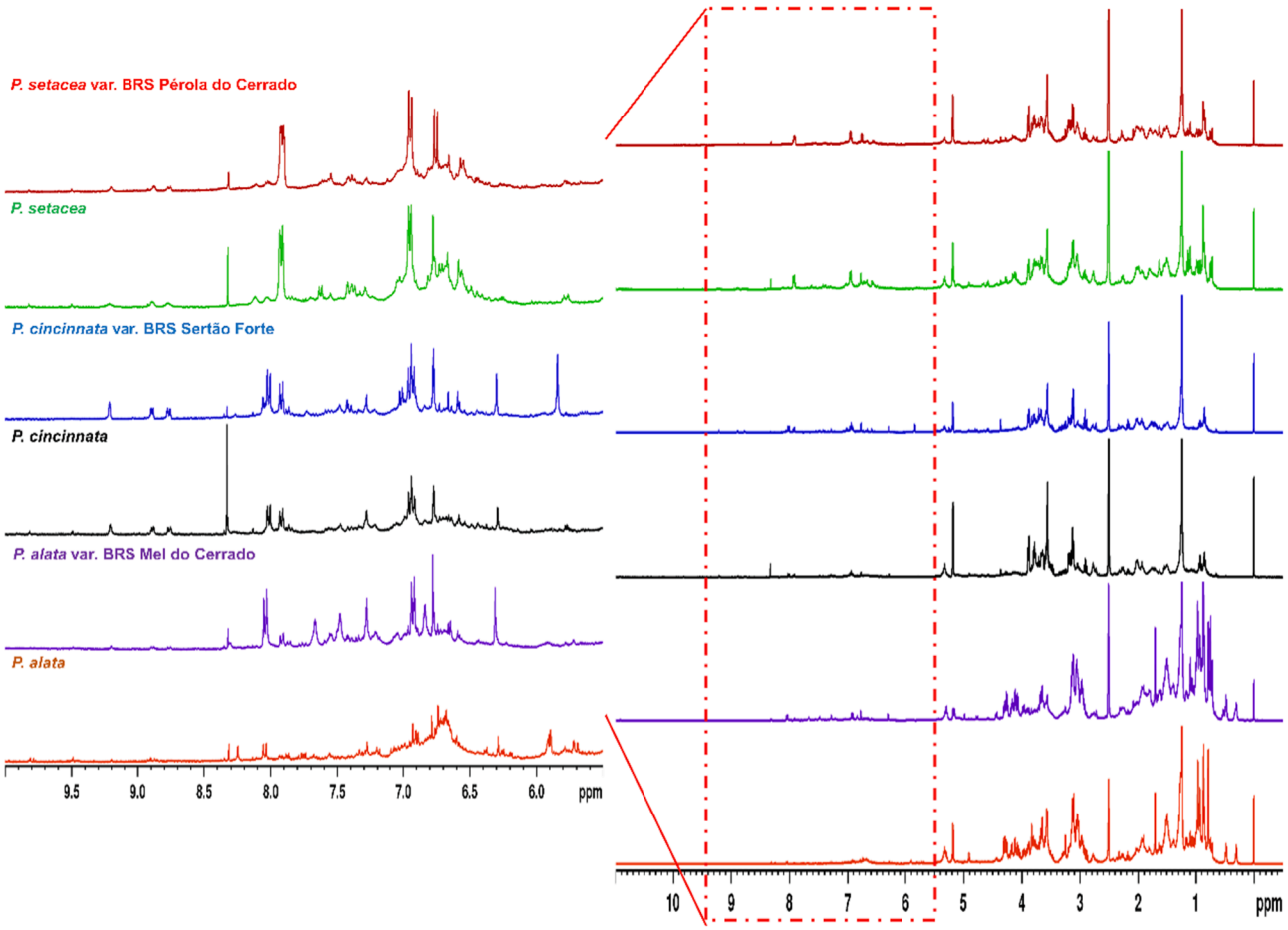

Fig. 1. ^{1}H NMR fingerprint of *Passiflora* extracts.

3. Results and discussion

3.1. Identification of metabolites in Passiflora extracts by 1D and 2D NMR experiments

The ^{1}H NMR metabolic profile allowed us to identify the main metabolites in the leaves ethanolic extracts of *Passiflora* species (Fig. 1 and Fig. 2). In all species investigated, the ^{1}H NMR spectra revealed a complex pattern of signals attributed to aliphatic (δ 0.50–3.00), glycosylated (δ 3.00–5.50), and aromatic compounds (δ 5.50–10.00) (Fig. 1). Signals attributed to primary and secondary metabolites in *Passiflora* species are depicted in Fig. 1 and detailed in Table 1S). Resonances associated with the presence of long-chain saturated fatty acids (**1**) were observed via signals at δ 1.48 (*m*, CH_2), δ 1.29–1.31 (*m*, CH_{2n}) – associated with methylene groups, δ 0.85 (*t*, $J = 6.5$ Hz, CH_3) – attributed to terminal methyl group of fatty acids, and a triplet at δ 2.17 (*t*, $J = 7.3$ Hz, CH_2), that showed long-range ^{1}H–^{13}C HMBC correlation map with the carbons at δ 24.7, 28.4 and 174.6. Also, unsaturated fatty acids (**2**) were identified by the signals at δ 0.92 (*t*, $J = 7.2$ Hz) and δ 5.06–5.38 associated respectively with the terminal methyl and olefinic hydrogens of these metabolites (Figs. 1 and 2, Table 1S). Fatty acids are typically found in nature, including in plants as *Passiflora* species (Farag et al., 2016).

The second region (δ 3.00–5.50) showed intense and overlapping signals related to the most abundant sugars and other anomeric hydrogens attributed to aglycones, typical of compounds in *Passiflora* species. α-glucose (**3**), β-glucose (**4**), and sucrose (**5**) were easily identified in all *Passiflora* extracts by tracking the anomeric hydrogens at δ 4.90 (*d*, $J =$ 3.6 Hz), δ 4.26 (*d*, $J = 7.7$ Hz), and δ 5.18 (*d*, $J = 3.7$ Hz) (Abd Ghafar et al., 2020; Farag et al., 2016). One-bond and long-range correlation maps ensured the compounds identification. (Figs. 1 and 2, Table 1S).

In addition to primary metabolites, the ^{1}H NMR metabolic profiles of *P. alata* and *P. alata* var. BRS Mel do Cerrado displayed signals consistent with saponins quadranguloside (**6**) and oleanolic acid-3-sophoroside (**7**). The quadranguloside (**6**) was confirmed by the singlets at δ 0.86 (*s*, H-18), δ 0.93 (*s*, H-28), δ 0.96 (*s*, H-29), and δ 0.78 (*s*, H-30) that, according to the ^{1}H–^{13}C HSQC experiment, are respectively attached to the carbons at δ 19.4 (C-18), 18.3 (C-28), 25.1 (C-29), and δ 14.9 (C-30).

Table 1
Overview of the metabolites identified in *Passiflora* extracts.

Metabolite	A	B	C	D	E	F
Saturated fatty acids (**1**)	x	x	x	x	x	x
Unsaturated fatty acids (**2**)	x	x	x	x	x	x
α-Glucose (**3**)	x	x	x	x	x	x
β-Glucose (**4**)	x	x	x	x	x	x
Sucrose (**5**)	x	x	x	x	x	x
Quadranguloside (**6**)	x	x				
Oleanolic acid-3-sophoroside (**7**)	x	x				
Isoorientin (**8**)				x		
Isovitexin (**9**)			x	x	x	x
Vitexin (**10**)	x	x				
Vitexin-2″-*O*-rhamnoside (**11**)	x	x				
Vitexin-2″-*O*-xyloside (**12**)			x	x		
Isovitexin-2″-*O*-xyloside (**13**)			x	x	x	x
Trigonelline (**14**)	x	x	x	x	x	x

A – *Passiflora alata*; **B** – *Passiflora alata* var. BRS Mel do Cerrado; **C** – *Passiflora cincinnata*; **D** – *Passiflora cincinnata* var. BRS Sertão Forte; **E** – *Passiflora setacea*; **F** – *Passiflora setacea* var. BRS Pérola do Cerrado.

The methyl groups at C-29 and C-30 showed long-range ^{1}H–^{13}C HMBC correlations with carbon at δ 87.4 (C-3) and its hydrogen at δ 3.12 (*m*, H-3). Likewise, the doublet at δ 4.17 (*d*, $J = 7.7$ Hz, H-1′) correlated with the carbon at δ 105.3 in the ^{1}H–^{13}C HSQC, as well as long-range ^{1}H–^{13}C HMBC with the carbon at δ 87.4, supporting the gentiobiose unit at C-3. The other methyl group, at δ 1.70 (*s*, H-27), revealed one-bond ^{1}H–^{13}C HSQC correlation map with the carbon at δ 21.6 and long-range ^{1}H–^{13}C HMBC correlation map with the carbons δ 66.4 (C-26), 130.2 (C-24), and 130.8C (C-25) of quadranguloside (**6**) (Doyama et al., 2005). The signal at δ 4.11 (*br s*, H-26) is attached to C-26, while the multiplet at δ 5.28 (*m*, H-24) is bonded to C-24. The doublets at δ 0.30 (*d*, $J = 3.8$ Hz) and δ 0.48 (*d*, $J = 3.8$ Hz) displayed one-bond ^{1}H–^{13}C HSQC correlation map with the carbons at δ 29.6 (C-19), also of quadranguloside (**6**) (Figs. 1 and 2, Table 1S). The saponin oleanolic acid-3-sophoroside (**7**) was characterized by the methyl hydrogens at δ 0.74 (*s*, H-23), δ 0.99 (*s*, H-24), δ 0.86 (*s*, H-25), δ 0.71 (*s*, H-26), δ 1.09 (*s*, H-27), and δ 0.87 (*s*, H-29 and H-30). The olefinic hydrogen at δ 5.15 (*br t*, H-12) showed one-bond ^{1}H–^{13}C HSQC with the carbon at δ 121.4. Furthermore, methyl groups

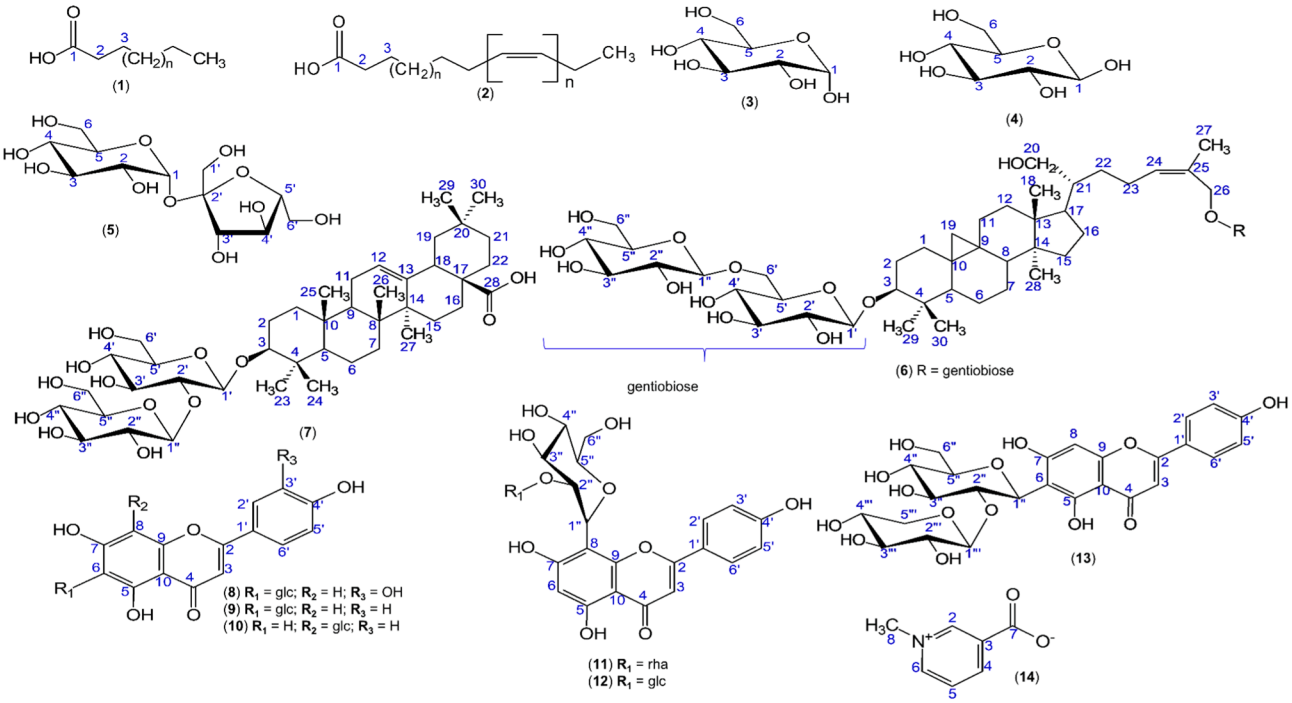

Fig. 2. Main metabolites identified in *Passiflora* extracts.

at C-23 and C-24 of oleanolic acid-3-sophoroside (**7**) exhibited $^{1}H–^{13}C$ HMBC correlation map with the signal at δ 88.3 (C-3), which is attached to hydrogen at δ 3.04 (*m*, H-3). Also, the doublet at δ 4.25 (*d*, $J = 7.8$ Hz, H-1′) showed $^{1}H–^{13}C$ HMBC with the carbon at 88.3, confirming the glycosidic unit at C-3 (Doyama et al., 2005). The other glycosidic unit of oleanolic acid-3-sophoroside (**7**) was attributed based on the anomeric hydrogen at δ 4.43 (*d*, $J = 7.8$ Hz, H-1″) (Figs. 1 and 2, Table 1S).

The aromatic region (δ 5.50 to 10.00) revealed the presence of flavonoids and alkaloids, often found in species of the genus *Passiflora* (Fig. 1). Flavonoids are the most abundant class of secondary metabolites present in this genus and possess diverse medicinal properties, which explains their use as chemical markers for quality control of *Passiflora* species (Dhawan et al., 2004; Patel et al., 2011; Tremmel, Kiermaier, & Heilmann, 2021). Isoorientin (**8**) was identified in the ^{1}H NMR metabolic profile of *P. cincinnata* var. BRS Sertão Forte trough the signals at δ 6.58 (s, H-8) and δ 6.66 (s, H-3) that exhibited one-bond $^{1}H–^{13}C$ HSQC correlation map with carbons at δ 93.6 (C-8) and 102.8 (C-3), respectively – which is consistent to the rings A and C of a 5,6,7-trisubstituted flavone – and anomeric hydrogen at δ 4.59 (*d*, $J = 9.8$ Hz, H-1″). Also, an ABX system was observed at δ 6.92 (*d*, $J = 8.3$ Hz, H-2′) and δ 7.43 (*d*, $J = 2.3$ Hz, H-5′) and a double of doublets at δ 7.40 (*dd*, $J = 8.3$ and 2.3 Hz, H-6′) in accordance to 3′,4′-disubstituted ring B (Figs. 1 and 2, Table 1S) (Ferreira et al., 2016). The derivative of 6-C-glycosylated flavone of apigenin, known as isovitexin (**9**) was observed in the ^{1}H NMR metabolic profile of all *Passiflora* extracts, except for *P. alata* and its genetic variety (Figs. 1 and 2, Table 1S). In contrast to **8**, isovitexin (**9**) showed two doublets at δ 7.91 (d, $J = 8.8$ Hz, H-2′/H-6′) and δ 6.95 (*d*, $J = 8.8$ Hz, H-3′/H-5′), typical AA'BB' coupling system of the ring B. The singlet at δ 6.60 (*s*, H-8) showed one-bond $^{1}H–^{13}C$ HSQC correlation map with the carbon at δ 93.7 (C-8). The signal at δ 6.76 (*s*, H-3) displayed a long-range $^{1}H–^{13}C$ HMBC correlation map with the carbons at δ 103.4 (C-10), δ 121.6 (C-1′), δ 163.5 (C-2), and δ 181.9 (C-4), supporting the hydrogen at C-3. The anomeric hydrogen in the isovitexin (**9**) was confirmed with the presence of doublet at δ 4.58 (*d*, $J = 9.8$ Hz, H-1″), which showed $^{1}H–^{13}C$ HSQC correlation map with the carbon at δ 73.0 and $^{1}H–^{13}C$ HMBC correlation map with the carbons at δ 160.4 (C-5), δ 108.7 (C-6) and δ 163.2 (C-7) of the flavone ring A (Ferreira et al., 2016; Hosoya et al., 2005).

Vitexin (**10**) and vitexin-2″-*O*-rhamnoside (**11**) were identified in *P. alata* and *P. alata* var. BRS Mel do Cerrado. The flavone **10** was characterized by the resonances at δ 6.30 (*s*, H-6) and δ 6.76 (*s*, H-3). Just as for isovitexin, it was observed an AA'BB' coupling system at δ 7.91 (*d*, $J = 8.8$ Hz, H-2′/H-6′) and δ 6.94 (*d*, $J = 8.8$ Hz, H-3′/ H-5′). The anomeric hydrogen of glucose attached at C-8 was observed at δ 4.76 (*d*, $J = 9.9$ Hz, H-1″) (Farag et al., 2016; Ferreira et al., 2016). Evidence of this fact is the long-range $^{1}H–^{13}C$ HMBC correlation of the anomeric hydrogen (H-1″) with carbons at δ 162.6 (C-7), δ 104.8 (C-8), and δ 155.9 (C-9), confirming the 5,7,8-trisubstituted flavone (Figs. 1 and 2., Table 1S). Vitexin-2″-*O*-rhamnoside (**11**) revealed the presence of resonances at δ 4.76 (*d*, $J = 9.8$ Hz, H-1″) and δ 4.98 (*br s*, H-1‴) and their one-bond correlations with carbons at 71.6 (C-1″) and 100.1 (C-1‴), respectively, which are characteristic of glucose and rhamnose units (Ferreira et al., 2016). The doublet at δ 0.48 (*d*, $J = 6.2$ Hz, H-6‴) attached to C-6″ (δ 17.3) confirmed the presence of the rhamnose unit. The two singlets at δ 6.31 (*s*, H-6) and δ 6.77 (s, H-3), as well as, two doublets of an AA'BB' coupling system at δ 8.04 (*d*, $J = 8.7$ Hz, H-2′/H-6′) and δ 6.93 (*d*, $J = 8.7$ Hz, H-3′/H-5′), confirmed the presence of **11** (Figs. 1 and 2, Table 1S).

The ^{1}H NMR metabolic profiling of the *P. cincinnata* extract and its genetic variety revealed two doublets at δ 8.01 (*d*, $J = 8.8$ Hz, H-2′/H-6′) and δ 6.92 (d, $J = 8.8$ Hz, H-3′/H-5′) - typical of an AA'BB' system of the ring B of a flavone - as well as two singlets at δ 6.30 (s, H-6) and δ 6.77 (s, H-3) that are relative to rings A and C of flavones. Anomeric hydrogens of glucose and xylose appeared at δ 4.79 (*d*, $J = 9.8$ Hz, H-1″) and δ 3.88 (*d*, $J = 8.0$ Hz, H-1‴) along with their carbons at δ 71.1 and δ 105.8, respectively, corroborating the presence of vitexin-2″-*O*-xyloside (**12**) (Figs. 1 and 2., Table 1S) (Gazola et al., 2018; Zielińska-Pisklak et al., 2014). Except for *P. alata* and its genetic variety, the ^{1}H NMR metabolic profile of the *Passiflora* species studied presented signals similar to vitexin-2″-*O*-xyloside (**12**), differing only in the position of the glycosidic unit. In these samples, it was observed the presence of a singlet at δ 6.57 (*s*, H-8) and its carbon at δ 93.6, which showed long-range $^{1}H–^{13}C$ HMBC correlation map with the carbons δ 107.8 (C-6), δ 163.6 (C-7), 156.4 (C-9), and 103.2 (C-10), characteristic of the ring A of the flavonoid; as well as the signal at δ 6.77 (s, H-3) and its carbon signal at δ 102.7. The ring B, in turn, was identified via doublets at δ 7.92 (*d*, $J = 8.6$ Hz, H-2′/H-6′) and δ 6.95 (*d*, $J = 8.6$ Hz, H-3′/ H-5′), indicating an AA'BB' coupling system. Also, two doublets were observed at δ 4.66 (*d*, $J = 9.8$ Hz, H-1″) and δ 4.14 (*d*, $J = 8.4$ Hz, H-1‴), attached to carbons at δ 71.2 and δ 105.4, characteristic of anomeric hydrogens of glucose and xylose, respectively. The signal at 4.66 (H-1″) showed long-range HMBC correlation map with the carbons at δ 160.9 (C-5) and δ 107.8 (C-6), from isovitexin-2″-*O*-xyloside (**13**) (Figs. 1 and 2, Table 1S) (Gazola et al., 2018; Zielińska-Pisklak et al., 2014).

In addition, the alkaloid trigonelline (**14**) was identified in all *Passiflora* species by the existence of the singlet at δ 9.21 (*s*, H-2), two doublets at δ 8.76 (*d*, $J = 7.9$ Hz, H-4) and δ 8.89 (*d*, $J = 6.0$ Hz, H-6), a double doublet at δ 8.03 (*dd*, $J = 7.9$ and 6.0 Hz, H-5), and a methyl group at δ 4.36 (*s*, CH_3-8) (Figs. 1 and 2., Table 1S) (Abd Ghafar et al., 2020; Farag et al., 2016). The trigonelline (**14**) was more pronounced in *P. cincinnata* var. BRS Sertão Forte. All the metabolites reported have been observed in other *Passiflora* (Castellanos et al., 2020; Farag et al., 2016; Patel et al., 2011). An overview of the metabolites found in *Passiflora* extracts are depicted in Table 1.

3.2. Multivariate data analysis

The ^{1}H NMR-based metabolic profiles, along with principal component analysis (PCA), were used to discriminate *Passiflora* species (*P. alata*, *P. cincinnata*, *P. setacea*, *P. alata* var. BRS Mel do Cerrado, *P. cincinnata* var. BRS Sertão Forte, and *P. setacea* var. BRS Pérola do Cerrado). Scores and loading plots obtained through the PCA analysis are displayed in Fig. 3. The two first principal components (PCs) explained 69.01% of the maximum variation among the data matrix, in which PC1 represented 52.75%, while PC2 demonstrated an additional 16.26%. According to the scores plot, six groups can be clearly observed, where the samples of *P. setacea* and *P. setacea* var. BRS Pérola do Cerrado were clustered on the negative sides of PC1 and PC2, while *P. cincinnata* and *P. cincinnata* var. BRS Sertão Forte were distributed in the negative region of PC1 and positive region of PC2. On the other hand, samples of *P. alata* and *P. alata* var. BRS Mel do Cerrado were arranged in the positive region of PC1, however, *P. alata* was distributed on the positive side of PC2 and its genetic variety on the negative side of PC2. The analysis of the loadings plot allowed to identify metabolites responsible for the discrimination of *Passiflora* species, providing a comparative interpretation of samples in the function of the chemical composition (Fig. 3). Thus, the metabolites responsible for discriminating the *P. alata* samples and its genetic variety in positive PC1 were associated signals at δ 0.30 (*d*, $J = 3.8$ Hz, H-19a), δ 0.48 (*d*, $J = 3.8$ Hz, H-19b), δ 0.78 (*s*, H-30), δ 0.86 (*s*, H-18), δ 0.93 (*s*, H-28), δ 1.70 (*s*, H-27), δ 3.11 (*m*, H-3), δ 5.28 (*m*, H-24), δ 4.11 (*br s*, H-26), δ 4.17 (*d*, $J = 7.7$ Hz), attributed to the saponin quadranguloside (**6**). Separation of P. *alata* var. BRS Mel do Cerrado samples were influenced by hydrogens at δ 0.71 (*s*, H-26), δ 0.74 (*s*, H-23), δ 0.86 (*s*, H-25), δ 0.87 (*s*, H-29 and H-30), δ 1.09 (*s*, H-27), δ 3.04 (*m*, H-3), δ 4.25 (*d*, $J = 7.8$ Hz, H-1″) and δ 4.43 (*d*, $J = 7.8$ Hz, H-1″) of the saponin oleanolic acid-3-sophoroside (**7**) (Fig. 3). Previous research showed that metabolite **6** is restricted to a few species (Costa et al., 2016). Quadranguloside (**6**) has been reported as the major saponin of *P. alata* leaves (Reginatto, Gosmann, Schripsema, & Schenkel, 2004). Along with oleanolic acid-3-sophoroside (**7**), quadranguloside (**6**) was previously identified in *P. quadranqularis* (Dhawan et al., 2004; Doyama et al., 2005; Reginatto et al., 2001). The anxiolytic activity of

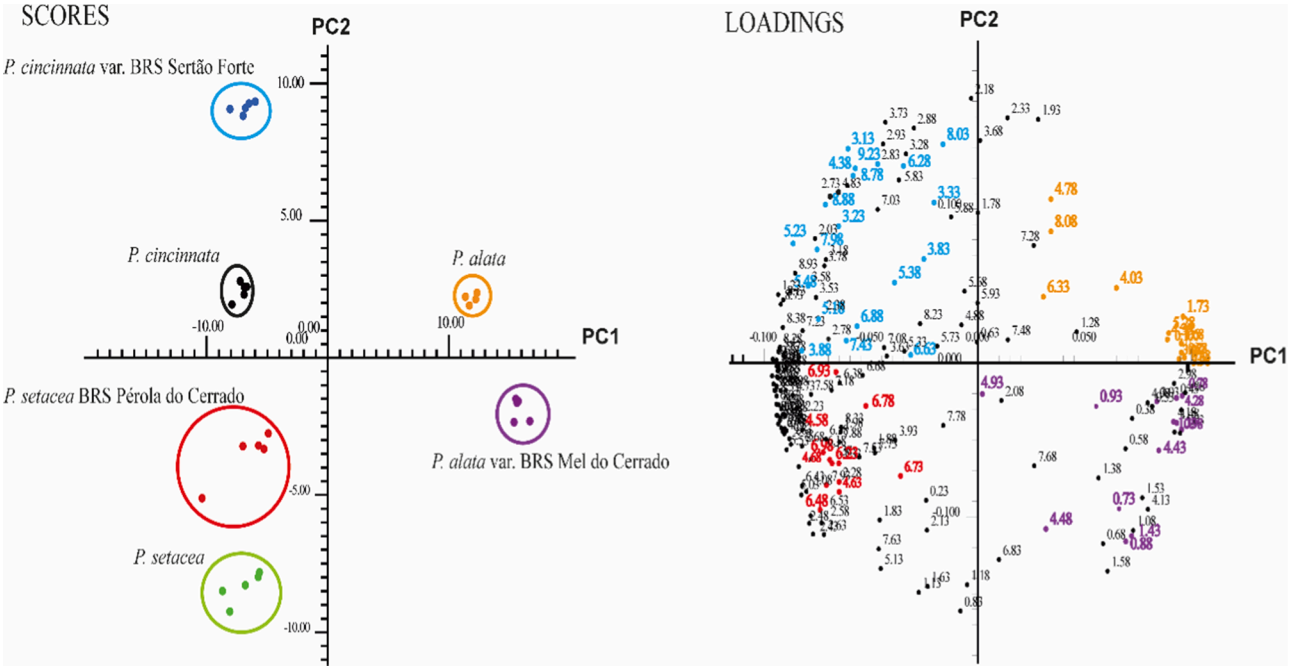

Fig. 3. Principal components analysis (PCA) of *Passiflora* showing PC1 (52.75%) versus PC2 (16.26%). Loadings plot of PC1 versus PC2 are also depicted, discriminating the compounds responsible for the separation of groups.

P. alata, has been mostly associated to quadranguloside (**6**), while vasoconstrictor effects has been attributed to oleanolic acid-3-sophoroside (**7**) (Bareño, Puebla, Feliciano, & Guerrero, 2020; Braga et al., 2013; Smruthi, Divya, Archana, & Ravi, 2020).

Furthermore, α-glucose (**3**) (4.90, *d*, $J = 3.6$ Hz, H-1) and β–glucose (**4**) (4.26, *d*, $J = 7.7$, H-1) also contributed to the distribution of *P. alata* var BRS Mel do Cerrado in the negative PC2 (Fig. 3). Metabolomic studies have showed the isomeric forms of the glucose in *Passiflora* species (Daza et al., 2021; Farag et al., 2016). In addition to the signals related to quadranguloside (**6**), vitexin-2-*O*"-rhamnoside (**11**) was the metabolite responsible for bringing *P. alata* samples to positive sides of PC1 and PC2 due to signals at δ 4.07 (*d*, $J = 7.7$ Hz, H-2″), δ 4.76 (*d*, $J =$ 9.8, H-1″), δ 6.31 (*s*, H-6), and δ 8.04 (*d*, $J = 8.7$ Hz, H-2′ and H-6′) of the hydrogens in C-2″, C-1″, C-6, C-2′, C-6′ of **11** (Fig. 3). This flavone has been also identified in other *Passiflora* species (*P. alata*, *P. foetida*, and *P. biflora*) and has exhibited antioxidant activity (Chiavaroli et al., 2020; Costa et al., 2016; Doyama et al., 2005; Rosa et al., 2021; Zucolotto et al., 2012).

The loadings plot showed samples of *P. setacea* and *P. setacea* var. BRS Pérola do Cerrado in the negative regions of PC1 and PC2 as consequence of signals at δ 4.66 (*d*, $J = 9.8$ Hz, H-1″), δ 6.57 (*s*, H-8), δ 6.77 (*s*, H-3), δ 6.95 (*d*, $J = 8.6$ Hz, H-3′ and H-5′), and δ 7.92 (*d*, $J = 8.6$ Hz, H-2′and H-6′) of the isovitexin-2-*O*"-xyloside (**13**). The separation was also influenced by signals of the flavone isovitexin (**9**), such as δ 4.58 (*d*, $J = 9.8$ Hz, H-1″), δ 6.60 (*s*, H-8), δ 6.76 (*s*, H-3), and δ 6.95 (*d*, J = 8.8 Hz, H-3′ and H-5′) (Fig. 3). Flavone **9** has been described in many *Passiflora* species - including *P. alata*, *P. cincinnata*, *P. edulis*, *P. quadrangulares*, *P. incarnata*, and *P. setacea* (Doyama et al., 2005; Francischini, Lopes, Segatto, Stahl, & Zuin, 2020; Noriega & de Mafud, 2011; Wosch et al., 2017) - and several biological effects have been associated to it, notably as antioxidant, antidepressant, antinociceptive, neuroprotective, cardioprotective, and anti-inflammatory activities (Azubuike-Osu, Ohanenye, Jacob, Ejike, & Udenigwe, 2020; He et al., 2016). Moreover, the isovitexin-2-*O*"-xyloside (**13**) has been reported in *P. serratifolia* and *P. quadrangularis* (Farag et al., 2016). The pharmacological action of compound **13** is still unclear. Signals with low intensities associated with other aromatic compounds also showed an important contribution to the discrimination of *P. setacea* and *P. setacea* var. BRS Pérola do Cerrado, as well as signals attributed to aliphatic compounds, which may be related to the presence of other flavonoids, terpenoids, and amino acids; commonly found in species of the genus *Passiflora* (Daza et al., 2021; Farag et al., 2016; Flores et al., 2020).

In contrast, the *P. cincinnata* samples and its genetic variety were arranged in PC1 negative and PC2 positive due to the hydrogens attached to C-1″, C-6, C-2′ and C-6′ of the vitexin-2-*O*"-xyloside (**12**) at δ 3.88 (*d*, $J = 8.0$ Hz, H-1″), δ 8.01 (*d*, $J = 8.0$ Hz, H-2′ and H-6′) and δ 6.30 (*s*, H-6), respectively (Fig. 3). The presence of that flavone (**12**) has been reported in *P. quadrangularis* and *P. foetida*. Among the biologic activities reported to compound **13** includes sedative, antioxidant, and anti-proliferative (Gazola et al., 2018; Nguyen et al., 2015; Ninfali & Angelino, 2013; Wen, Zhao, Jiang, Yu, Zeng, Yang, & Yang, 2017). As vitexin-2-*O*"-xyloside (**12**), isoorientin (**8**) was relevant for the discrimination of *P. cincinnata* and *P. cincinnata* var. BRS Sertão Forte trough the signals at δ 6.92 (*d*, $J = 8.3$ Hz, H-5′), δ 7.40 (*dd*, $J = 8.3$ and 2.3 Hz, H-6′), δ 7.43 (*d*, $J = 2.3$ Hz, H-2′), and δ 6.66 (*s*, H-8) (Fig. 3). The isoorientin (**8**) has been recognized for its promising anti-inflammatory (Lee, Ku, & Bae, 2014), antioxidant (da Morrone, 2013), antidiabetic and antiplatelet activities (Salles et al., 2019), and has been identified in several *Passiflora* species (Alves et al., 2020; da Morrone, 2013; Patel et al., 2011; Salles et al., 2019; Schäfer et al., 2020), including as *P. alata*, *P. cincinnata*, and *P. setacea* (de Carvalho, de Oliveira, & de L., & Costa, A. M., 2018; Wosch et al., 2017).

Sucrose (**5**) also contributed to this discrimination of *P. cincinnata* and *P. cincinnata* var. BRS Sertão Forte, mainly because of the signal at δ 5.18 (*d*, $J = 3.7$ Hz, H-1) (Fig. 3). In addition to **5**, **8** and **12**, signals associated with saturated fatty acids (**1**), and olefinic hydrogens of unsaturated fatty acids (**2**) showed relevant in the differentiation of *P. cincinnata* and *P. cincinnata* var. BRS Sertão Forte. Likewise, trigonelline (**14**) influenced in the differentiation of *P. cincinnata* due hydrogens to the pyridine alkaloid at δ 4.36 (*s*, CH_3-8), δ 8.03 (*dd*, $J = 7.9$ and 6.0 Hz, H-5), δ 8.76 (*d*, $J = 7.9$ Hz, H-4), δ 8.89 (*d*, $J = 6.0$ Hz, H-6), and δ 9.21 (*s*, H-2) (Fig. 3) (Abd Ghafar et al., 2020; Castellanos et al., 2020; Girelli et al., 2018; da Santos, 2018).

The flavonoids played an important role in the discrimination of *Passiflora* samples. Those compounds have been strongly correlated with the bioactivity of *Passiflora* species and tracking them is essential to

evaluate the quality control of these matrix. However, working with chemical profiles, as proposed here, can be more effective in such purpose since it allows analyzing multiple compounds that synergically can be responsible for the final bioactivity.

4. Conclusion

A total of 14 compounds – from different chemical classes: carbohydrates, fatty acids, saponins, alkaloids, and mainly flavonoids - were identified in the ^{1}H NMR metabolic profiles of *Passiflora* species and their genetic varieties. Saturated and unsaturated fatty acids, α-glucose, β-glucose, sucrose, and trigonelline were found in all species investigated. The discrimination of *Passiflora* species was achieved with clear separation between samples of *P. alata*, *P. setacea*, and *P. cincinnata* and flavonoids were mainly responsible for the samples' grouping. Quadranguloside, oleanolic acid-3-sophoroside, *α*-glucose, *β*-glucose, and vitexin-2-*O*"-rhamnoside were relevant in the differentiation of *P. alata* and *P. alata* var. BRS Pérola do Cerrado, while the flavones isovitexin and isovitexin-2-*O*"-xyloside were dominant in the grouping of *P. setacea* and *P. setacea* var. BRS Pérola do Cerrado, and finally *P. cincinnata* and *P. cincinnata* var. BRS Sertão Forte were influenced by the fatty acids, sucrose, flavones (isoorientin and vitexin-2-*O*"-xyloside), and alkaloid trigonelline. No differences were observed in the chemical profiles of *P. setacea* and *P. cincinnata* with their respective genetic varieties. However, discrimination was clearly saw by observed between *P. alata* and *Passiflora alata* Curtis var. BRS Mel do Cerrado and oleanolic acid-3-sophoroside influenced such separation.

Passiflora species are often used for the same therapeutic applications, however this study indicated heterogeneous metabolite profiles, and this fact can cause therapeutic effectiveness variation. The multiple compound approach, as adopted in this paper, can be efficient for quality control evaluation, and contribute to the investigation of alternatives for official *Passiflora* herbal medicines.

Declaration of Competing Interest

The authors declare that they have no known competing financial interests or personal relationships that could have appeared to influence the work reported in this paper.

Data availability

No data was used for the research described in the article.

Acknowledgements

The authors gratefully acknowledge to CAPES, CNPq, FACEPE, UFAM, UNIVASF and EMBRAPA for the financial support. Dutra is grateful to CAPES for his postdoctoral scholarships (88882.317992/2019-01). The authors thank to Conselho Nacional de Desenvolvimento Científico e Tecnológico – CNPq (Process 431566/2018-6 and 307782/2017-4) for financial support.

References

Abd Ghafar, S. Z., Mediani, A., Maulidiani, M., Rudiyanto, R., Mohd Ghazali, H., Ramli, N. S., & Abas, F. (2020). Complementary NMR- and MS-based metabolomics approaches reveal the correlations of phytochemicals and biological activities in *Phyllanthus acidus* leaf extracts. *Food Research International, 136*(April), Article 109312. https://doi.org/10.1016/j.foodres.2020.109312

Alves, J. S. F., Dos Santos Silva, A. M., Da Silva, R. M., Tiago, P. R. F., De Carvalho, T. G., De Araújo Júnior, R. F., … Zucolotto, S. M. (2020). *In vivo* antidepressant effect of *Passiflora edulis* f. Flavicarpa into cationic nanoparticles: Improving bioactivity and safety. *Pharmaceutics, 12*(4). https://doi.org/10.3390/pharmaceutics12040383

Anvisa. (2019). Farmacopeia Brasileira. 6a Edição. *Anvisa*, *1*, 874.

Anvisa (2021). *Formulário de Fitoterápicos Agência Nacional de Vigilância Sanitária-Anvisa 2ª EDIÇÃO*. Retrieved from https://www.gov.br/anvisa/pt-br.

Azubuike-Osu, S. O., Ohanenye, I. C., Jacob, C., Ejike, C. E. C. C., & Udenigwe, C. C. (2020). Beneficial role of vitexin and isovitexin flavonoids in the vascular endothelium and cardiovascular system. *Current Nutraceuticals, 01*, 127–134. https://doi.org/10.2174/2665978601999201105160405

Bareño, L. L., Puebla, P., Feliciano, A. S. A. N., & Guerrero, M. F. (2020). Vascular mechanisms of monodesmosidic triterpene saponins isolated from *Passiflora quadrangularis* L. *Vitae, 27*(2), 1–11. https://doi.org/10.17533/udea.vitae.v27n2a02

Bernardes, P. M., Nicoli, C. F., Alexandre, R. S., Guilhen, J. H. S., Praça-Fontes, M. M., Ferreira, A., & da Silva Ferreira, M. F. (2020). Vegetative and reproductive performance of species of the genus *Passiflora*. *Scientia Horticulturae, 265*(November 2019). https://doi.org/10.1016/j.scienta.2020.109193

Bomtempo, L. L., Costa, A. M., Lima, H., Engeseth, N., & Gloria, M. B. A. (2016). Bioactive amines in *Passiflora* are affected by species and fruit development. *Food Research International, 89*, 733–738. https://doi.org/10.1016/j.foodres.2016.09.028

Braga, A., Cristina Stein, A., Dischkaln Stolz, E., Dallegrave, E., Buffon, A., Do Rego, J. C., … Kuze Rates, S. M. (2013). Repeated administration of an aqueous spray-dried extract of the leaves of *Passiflora alata* Curtis (Passifloraceae) inhibits body weight gain without altering mice behavior. *Journal of Ethnopharmacology, 145*(1), 59–66. https://doi.org/10.1016/j.jep.2012.10.034

Brahmi, F., Nguyen, A. T., Nacoulma, A. P., Sheridan, H., Wang, J., Guendouze, N., … Duez, P. (2020). Discrimination of *Mentha* species grown in different geographical areas of Algeria using ^{1}H-NMR-based metabolomics. *Journal of Pharmaceutical and Biomedical Analysis, 189*. https://doi.org/10.1016/j.jpba.2020.113430

Castellanos, L., Naranjo-Gaybor, S. J., Forero, A. M., Morales, G., Wilson, E. G., Ramos, F. A., & Choi, Y. H. (2020). Metabolic fingerprinting of banana passion fruits and its correlation with quorum quenching activity. *Phytochemistry, 172*(June 2019). https://doi.org/10.1016/j.phytochem.2020.112272

Chiavaroli, A., Di Simone, S. C., Sinan, K. I., Ciferri, M. C., Flores, G. A., Zengin, G., … Orlando, G. (2020). Pharmacological properties and chemical profiles of *Passiflora foetida* L. Extracts: Novel insights for pharmaceuticals and nutraceuticals. *Processes, 8*(9), 12886–12900. https://doi.org/10.3390/pr8091034

Costa, G. M., Gazola, A. C., Zucolotto, S. M., Castellanos, L., Ramos, F. A., Reginatto, F. H., & Schenkel, E. P. (2016). Chemical profiles of traditional preparations of four South American *Passiflora* species by chromatographic and capillary electrophoretic techniques. *Revista Brasileira de Farmacognosia, 26*(4), 451–458. https://doi.org/10.1016/j.bjp.2016.02.005

Danek, M., Plonka, J., & Barchanska, H. (2021). Metabolic profiles and non-targeted LC–MS/MS approach as a complementary tool to targeted analysis in assessment of plant exposure to pesticides. *Food Chemistry, 356*(March), Article 129680. https://doi.org/10.1016/j.foodchem.2021.129680

Daza, G. M., Macías, C. M., Forero, A. M., Rodríguez, J., Aragón, M., Jiménez, C., … Castellanos, L. (2021). Identification of α-amylase and α-glucosidase inhibitors and Ligularoside A, a new triterpenoid saponin from *Passiflora ligularis* Juss (Sweet Granadilla) leaves, by a nuclear magnetic resonance-based metabolomic study. *Journal of Agricultural and Food Chemistry, 69*(9), 2919–2931. https://doi.org/10.1021/acs.jafc.0c07850

de Carvalho, M. V. O., de Oliveira, L., & de L., & Costa, A. M.. (2018). Effect of training system and climate conditions on phytochemicals of *Passiflora setacea*, a wild *Passiflora* from Brazilian savannah. *Food Chemistry, 266*(November 2017), 350–358. https://doi.org/10.1016/j.foodchem.2018.05.097

Dhawan, K., Dhawan, S., & Sharma, A. (2004). Passiflora: A review update. *Journal of Ethnopharmacology, 94*(1), 1–23. https://doi.org/10.1016/j.jep.2004.02.023

Doyama, J. T., Rodrigues, H. G., Novelli, E. L. B., Cereda, E., & Vilegas, W. (2005). Chemical investigation and effects of the tea of *Passiflora alata* on biochemical parameters in rats. *Journal of Ethnopharmacology, 96*(3), 371–374. https://doi.org/10.1016/j.jep.2004.06.021

Dutra, L. M., da Conceição Santos, A. D., Lourenço, A. V. F., Nagata, N., Heiden, G., Campos, F. R., & Barison, A. (2020). ^{1}H HR-MAS NMR and chemometric methods for discrimination and classification of *Baccharis* (Asteraceae): A proposal for quality control of *Baccharis trimera*. *Journal of Pharmaceutical and Biomedical Analysis, 184*. https://doi.org/10.1016/j.jpba.2020.113200

Emwas, A. H., Roy, R., McKay, R. T., Tenori, L., Saccenti, E., Nagana Gowda, G. A., … Wishart, D. S. (2019). NMR spectroscopy for metabolomics research. *Metabolites, 9*(7). https://doi.org/10.3390/metabo9070123

Faleiro, F. G., Junqueira, N. T. V., Junghans, T. G., de Jesus, O. N., Miranda, D., & Otoni, W. C. (2019). Advances in passion fruit (*Passiflora* spp.) propagation. *Revista Brasileira de Fruticultura, 41*(2), 1–17. https://doi.org/10.1590/0100-29452019155

Farag, M. A., Otify, A., Porzel, A., Michel, C. G., Elsayed, A., & Wessjohann, L. A. (2016). Comparative metabolite profiling and fingerprinting of genus *Passiflora* leaves using a multiplex approach of UPLC-MS and NMR analyzed by chemometric tools. *Analytical and Bioanalytical Chemistry, 408*(12), 3125–3143. https://doi.org/10.1007/s00216-016-9376-4

Ferreira, R. O., De Carvalho Junior, A. R., Riger, C. J., Castro, R. N., Da Silva, T. M. S., & De Carvalho, M. G. (2016). Constituintes químicos e atividade antioxidante in vivo de flavonoides isolados de *Clusia lanceolata* (Clusiaceae). *Quimica Nova, 39*(9), 1093–1097. https://doi.org/10.21577/0100-4042.20160131

Figueiredo, D., Colomeu, T. C., Schumacher, N. S. G., Stivanin-Silva, L. G., Cazarin, C. B. B., Meletti, L. M. M., … Zollner, R. L. (2016). Aqueous leaf extract of *Passiflora alata* Curtis promotes antioxidant and anti-inflammatory effects and consequently preservation of NOD mice beta cells (non-obese diabetic). *International Immunopharmacology, 35*, 127–136. https://doi.org/10.1016/j.intimp.2016.03.031

Flores, I. S., Martinelli, B. C. B., & Lião, L. M. (2020). High-resolution magic angle spinning nuclear magnetic resonance (HR-MAS NMR) as a tool in the determination of biomarkers of *Passiflora*-based herbal medicines. *Fitoterapia, 142*(November 2019), Article 104500. https://doi.org/10.1016/j.fitote.2020.104500

Fonseca, L. R. d., Rodrigues, R. de A., Ramos, A. de S., Da Cruz, J. D., Ferreira, J. L. P., Silva, J. R. de A., & Amaral, A. C. F. (2020). Herbal Medicinal Products from

Passiflora for Anxiety: An Unexploited Potential. *Scientific World Journal*, *2020*. https://doi.org/10.1155/2020/6598434.

Francischini, D. S., Lopes, A. P., Segatto, M. L., Stahl, A. M., & Zuin, V. G. (2020). Development and application of green and sustainable analytical methods for flavonoid extraction from *Passiflora* waste. *BMC Chemistry, 14*(1), 1–11. https://doi.org/10.1186/s13065-020-00710-5

Gazola, A. C., Costa, G. M., Zucolotto, S. M., Castellanos, L., Ramos, F. A., de Lima, T. C. M., & Schenkel, E. P. (2018). The sedative activity of flavonoids from *Passiflora quadrangularis* is mediated through the GABAergic pathway. *Biomedicine and Pharmacotherapy, 100*(43), 388–393. https://doi.org/10.1016/j.biopha.2018.02.002

Girelli, C. R., Accogli, R., Del Coco, L., Angilè, F., De Bellis, L., & Fanizzi, F. P. (2018). ^{1}H-NMR-based metabolomic profiles of different sweet melon (*Cucumis melo* L.) Salento varieties: Analysis and comparison. *Food Research International, 114*(March), 81–89. https://doi.org/10.1016/j.foodres.2018.07.045

He, M., Min, J. W., Kong, W. L., He, X. H., Li, J. X., & Peng, B. W. (2016). A review on the pharmacological effects of vitexin and isovitexin. *Fitoterapia, 115*, 74–85. https://doi.org/10.1016/j.fitote.2016.09.011

He, X., Luan, F., Yang, Y., Wang, Z., Zhao, Z., Fang, J., … Li, Y. (2020). *Passiflora edulis*: An insight into current researches on phytochemistry and pharmacology. *Frontiers in Pharmacology, 11*(May), 1–16. https://doi.org/10.3389/fphar.2020.00617

Hellal, K., Mediani, A., Ismail, I. S., Tan, C. P., & Abas, F. (2021). ^{1}H NMR-based metabolomics and UHPLC-ESI-MS/MS for the investigation of bioactive compounds from *Lupinus albus* fractions. *Food Research International, 140(July*, 2020). https://doi.org/10.1016/j.foodres.2020.110046

Holanda, D. K. R., Wurlitzer, N. J., Dionisio, A. P., Campos, A. R., Moreira, R. A., de Sousa, P. H. M., … Costa, A. M. (2020). Garlic passion fruit (*Passiflora tenuifila* Killip): Assessment of eventual acute toxicity, anxiolytic, sedative, and anticonvulsant effects using *in vivo* assays. *Food Research International, 128(April*, 2019). https://doi.org/10.1016/j.foodres.2019.108813

Hosoya, T., Young, S. Y., & Kunugi, A. (2005). Five novel flavonoids from W*asabia japonica*. *Tetrahedron, 61*(29), 7037–7044. https://doi.org/10.1016/j.tet.2005.04.061

IBGE (2020). Produção agrícola municipal. Retrieved from Instituto Brasileiro de Geografia e Estatistica website: https://sidra.ibge.gov.br/tabela/5457.

Kim, H. K., Choi, Y. H., & Verpoorte, R. (2010). NMR-based metabolomic analysis of plants. *Nature Protocols, 5*(3), 536–549. https://doi.org/10.1038/nprot.2009.237

Lee, W., Ku, S. K., & Bae, J. S. (2014). Vascular barrier protective effects of orientin and isoorientin in LPS-induced inflammation *in vitro* and *in vivo*. *Vascular Pharmacology, 62*(1), 3–14. https://doi.org/10.1016/j.vph.2014.04.006

Marchesine, A. M., Prado, G. G., Messiano, G. B., Machado, M. B., & Lopes, L. X. L. (2009). Chemical Constituents of *Aristolochia giberti*. *Journal of the Brazilian Chemical Society, 20*(9), 1598–1608. https://doi.org/10.1590/S0103-50532009000900006

McCullagh, M., Goshawk, J., Eatough, D., Mortishire-Smith, R. J., Pereira, C. A., Yariwake, J. H., & Vissers, J. P. (2021). Profiling of the known-unknown *Passiflora* variant complement by liquid chromatography - Ion mobility - Mass spectrometry. *Talanta*, *221*(July 2020). https://doi.org/10.1016/j.talanta.2020.121311.

Morrone, M. da S., De Assis, A. M., Da Rocha, R. F., Gasparotto, J., Gazola, A. C., Costa, G. M., … Moreira, J. C. F. (2013). *Passiflora manicata* (Juss.) aqueous leaf extract protects against reactive oxygen species and protein glycation *in vitro* and *ex vivo* models. *Food and Chemical Toxicology*, *60*, 45–51. https://doi.org/10.1016/j.fct.2013.07.028.

Nguyen, T. Y., To, D. C., Tran, M. H., Lee, J. S., Lee, J. H., Kim, J. A., … Min, B. S. (2015). Anti-inflammatory flavonoids isolated from *Passiflora foetida*. *Natural Product Communications, 10*(6), 1–3. https://doi.org/10.1177/1934578X1501000634

Ninfali, P., & Angelino, D. (2013). Nutritional and functional potential of *Beta vulgaris* cicla and rubra. *Fitoterapia, 89*(1), 188–199. https://doi.org/10.1016/j.fitote.2013.06.004

Noriega, P., Mafud, D. de F., Strasser, M., Kato, E. T. M., & Bacchi, E. M. (2011). *Passiflora alata* Curtis: A brazilian medicinal plant. *Boletin Latinoamericano y Del Caribe de Plantas Medicinales y Aromaticas*, *10*(5), 398–413.

Ozarowski, M., Piasecka, A., Paszel-Jaworska, A., Chaves, D. S. de A., Romaniuk, A., Rybczynska, M., … Thiem, B. (2018). Comparison of bioactive compounds content in leaf extracts of *Passiflora incarnata*, *P. caerulea* and *P. alata* and *in vitro* cytotoxic potential on leukemia cell lines. *Revista Brasileira de Farmacognosia*, *28*(2), 179–191. https://doi.org/10.1016/j.bjp.2018.01.006.

Patel, S. S., Soni, H., Mishra, K., & Singhai, A. K. (2011). Recent updates on the genus *Passiflora*: A review. *International Journal of Research in Phytochemistry and Pharmacology, 1*(1), 1–16.

Pereira, P. P. A., Lima, L. K. S., Soares, T. L., Laranjeira, F. F., Jesus, O. N. de, & Girardi, E. A. (2019). Initial vegetative growth and survival analysis for the assessment of *Fusarium* wilt resistance in *Passiflora* spp. *Crop Protection*, *121*(September 2018), 195–203. https://doi.org/10.1016/j.cropro.2019.03.018.

Reginatto, F. H., Gosmann, G., Schripsema, J., & Schenkel, E. P. (2004). Assay of quadranguloside, the major saponin of leaves of *Passiflora alata*, by HPLC-UV. *Phytochemical Analysis, 15*(3), 195–197. https://doi.org/10.1002/pca.768

Reginatto, F. H., Kauffmann, C., Schripsema, J., Guillaume, D., Gosmann, G., & Schenkef, E. P. (2001). Steroidal and triterpenoidal glucosides from *Passiflora alata*. *Journal of the Brazilian Chemical Society, 12*(1), 32–36. https://doi.org/10.1590/S0103-50532001000100003

Rosa, L. C. da, Siqueira, M. R. P., Paumgartten, F. J. R., Pacheco, G., de Oliveira, E. A. M., de Moreira, D., & L.. (2021). Development and validation of a new method to quantify vitexin-2-O-rhamnoside on *Passiflora* L. extracts. *Journal of Medicinal Plants Research, 15*(1), 45–55. https://doi.org/10.5897/jmpr2020.7044

Salles, B. C. C., Silva, M. A., Taniguthi, L., Ferreira, J. N., Rocha, C. Q., Vilegas, W., … Paula, F. B. A. (2019). *Passiflora edulis* leaf extract: Evidence of antidiabetic and antiplatelet effects in rast. *(October)*. https://doi.org/10.1248/bpb.b18

Santos, A. D. da C., Fonseca, F. A., Dutra, L. M., Santos, M. de F. C., Menezes, L. R. A., Campos, F. R., … Barison, A. (2018). ^{1}H HR-MAS NMR-based metabolomics study of different persimmon cultivars (*Diospyros kaki*) during fruit development. *Food Chemistry*, *239*, 511–519. https://doi.org/10.1016/j.foodchem.2017.06.133.

Sasikala, V., Saravanan, S., & Parimelazhagan, T. (2011). Analgesic and anti-inflammatory activities of *Passiflora foetida* L. *Asian Pacific Journal of Tropical Medicine, 4*(8), 600–603. https://doi.org/10.1016/S1995-7645(11)60155-7

Schäfer, A. M., Gilgen, P. M., Spirgi, C., Potterat, O., Schwabedissen, M. Z., & H. e.. (2020). Constituents of *Passiflora incarnata*, but not of *Valeriana officinalis*, Interact with the Organic Anion Transporting Polypeptides (OATP)2B1 and OATP1A2. In. *Planta Medica* (Vol. 2). https://doi.org/10.1055/a-1305-3936

Shanmugam, S., Sandes, R. D. D., Rajan, M., Neta, M. T. S. L., dos Santos Lima, B., de Jesus, M. J. M., … de Souza Araújo, A. A. (2020). Volatile profiling and UHPLC-QqQ-MS/MS polyphenol analysis of *Passiflora leschenaultii* DC. fruits and its anti-radical and anti-diabetic properties. *Food Research International, 133*(March). https://doi.org/10.1016/j.foodres.2020.109202

Siebra, A. L. A., Oliveira, L. R., Martins, A. O. B. P. B., Siebra, D. C., Albuquerque, R. S., Lemos, I. C. S., … Kerntopf, M. R. (2018). Potentiation of antibiotic activity by *Passiflora cincinnata* Mast. front of strains *Staphylococcus aureus* and *Escherichia coli*. *Saudi Journal of Biological Sciences, 25*(1), 37–43. https://doi.org/10.1016/j.sjbs.2016.01.019

Smruthi, R., Divya, M., Archana, K., & Ravi, M. (2020). The active compounds of *Passiflora* spp and their potential medicinal uses from both in vitro and in vivo evidences. *Journal of Advanced Biomedical and Pharmaceutical Sciences*. https://doi.org/10.21608/jabps.2020.44321.1105

Snyder, D. A. (2021). Covariance NMR: Theoretical concerns, practical considerations, contemporary applications and related techniques. *Progress in Nuclear Magnetic Resonance Spectroscopy, 122*, 1–10. https://doi.org/10.1016/j.pnmrs.2020.09.001

Tremmel, M., Kiermaier, J., & Heilmann, J. (2021). *In vitro* metabolism of six c-glycosidic flavonoids from *Passiflora incarnata* L. *International Journal of Molecular Sciences, 22*(12). https://doi.org/10.3390/ijms22126566

Wasicky, A., Hernandes, L. S., Vetore-Neto, A., Moreno, P. R. H., Bacchi, E. M., Kato, E. T. M., & Yoshida, M. (2015). Evaluation of gastroprotective activity of *Passiflora alata*. *Revista Brasileira de Farmacognosia, 25*(4), 407–412. https://doi.org/10.1016/j.bjp.2015.07.011

Wen, L., Zhao, Y., Jiang, Y., Yu, L., Zeng, X., Yang, J., … Yang, B. (2017). Identification of a flavonoid C-glycoside as potent antioxidant. *Free Radical Biology and Medicine*, *110*(October 2016), 92–101. https://doi.org/10.1016/j.freeradbiomed.2017.05.027.

Wishart, D. S., Feunang, Y. D., Marcu, A., Guo, A. C., Liang, K., Vázquez-Fresno, R., … Scalbert, A. (2018). HMDB 4.0: The human metabolome database for 2018. *Nucleic Acids Research, 46*(D1), D608–D617. https://doi.org/10.1093/nar/gkx1089

Wosch, L., dos Santos, K. C., Imig, D. C., & Santos, C. A. M. (2017). Comparative study of *Passiflora* taxa leaves: II. A chromatographic profile. *Revista Brasileira de Farmacognosia, 27*(1), 40–49. https://doi.org/10.1016/j.bjp.2016.06.007

Zielińska-Pisklak, M. A., Kaliszewska, D., Stolarczyk, M., & Kiss, A. K. (2014). Activity-guided isolation, identification and quantification of biologically active isomeric compounds from folk medicinal plant *Desmodium adscendens* using high performance liquid chromatography with diode array detector, mass spectrometry and multidiment. *Journal of Pharmaceutical and Biomedical Analysis, 102*, 54–63. https://doi.org/10.1016/j.jpba.2014.08.033

Zucolotto, S. M., Fagundes, C., Reginatto, F. H., Ramos, F. A., Castellanos, L., Duque, C., & Schenkel, E. P. (2012). Analysis of C-glycosyl flavonoids from South American *Passiflora* species by HPLC-DAD and HPLC-MS. *Phytochemical Analysis, 23*(3), 232–239. https://doi.org/10.1002/pca.1348